Raman Excitation Profiles of C_{70} in Benzene Solution. Assignment of the Electronic Spectrum in the 380−510-nm Region

Sean H. Gallagher,[†] Robert S. Armstrong,*[,†] Robert D. Bolskar,[‡] Peter A. Lay,*[,†] and Christopher A. Reed[‡]

Contribution from the School of Chemistry, University of Sydney, Sydney, New South Wales 2006, Australia, and Department of Chemistry, University of Southern California, Los Angeles, California 90089-0744

Received October 1, 1996[⊗]

Abstract: The resonance Raman (RR) spectrum of C_{70} has been studied in benzene using 11 laser excitation energies across the main visible absorption band (MVAB) of C_{70} between 514.5 and 406.7 nm. Raman excitation profiles (REPs) were constructed for the 15 most intense RR bands of C_{70}, and symmetry assignments have been made partly on the basis of polarization work. Contrast is made to work performed on thin films where problems have arisen from the symmetry-lowering effect of the surface and from neglect of resonance. Assignments for nine other less intense RR bands are suggested. Three electronic transitions under the MVAB are identified and assigned definitively: the HOMO − 4 (e_2'') → LUMO + 1 (e_1'') transition in the 514/501-nm excitation region, the HOMO − 5 (e_1') → LUMO + 1 (e_1'') transition in the 476/472-nm excitation region, and the HOMO (a_2'') → LUMO + 2 (a_1'') in the 457/452-nm excitation region. The REPs reveal that these three electronic transitions are vibronically coupled to the strong electronic transition at 382 nm which is assigned to the HOMO − 2 (a_2') → LUMO + 3 (e_1') transition. RR *B*-term scattering mechanisms are the major source of intensity enhancement for bands of the totally-symmetric A_1' and the non-totally-symmetric E_1'' and E_2' Raman modes. The REPs of the 15 bands are grouped into four types that provide insight into the change in the electronic distribution upon excitation for each transition. Unlike C_{60}, whose extraordinarily high symmetry makes it very sensitive to solvent-induced symmetry lowering and whose RR spectrum is rich in forbidden, overtone, and combination bands, C_{70} displays a restricted subset of RR scattering phenomena. The lower symmetry and more localized molecular orbitals of C_{70} make it a better model for the RR scattering mechanisms and vibronic coupling expected in the higher fullerenes.

Introduction

The insertion of a belt of 10 carbon atoms between two hemispheres of C_{60} creates C_{70}. The symmetry is lowered from I_h to D_{5h}, and this is manifest in three ways: vibrationally, there are a greater number of infrared and Raman vibrational features;[1−20] electronically, the first allowed transition has lower energy and the allowed transitions are more numerous;[21−23] and vibronically, the coupling of vibrational and electronic states is stronger and more extensive.[18]

C_{60} has 3-, 4-, and 5-fold degenerate vibrations whereas the vibrations of C_{70} are at most doubly-degenerate. Because the lower symmetry of C_{70} is closer to those of the heavier members of the fullerene family, C_{70} should be a better model than C_{60} for the vibrational and vibronic properties of the higher fullerenes. At the same time, C_{60} can provide valuable information about the vibrational dynamics of C_{70} because of

[†] University of Sydney.
[‡] University of Southern California.
[⊗] Abstract published in *Advance ACS Abstracts,* April 15, 1997.

(1) Taylor, R.; Hare, J. P.; Abdul-Sada, A. K.; Kroto, H. W. *J. Chem. Soc., Chem. Commun.* **1990**, 1423−1425.
(2) Hare, J. P.; Dennis, T. J.; Kroto, H. W.; Taylor, R.; Allaf, A. W.; Balm, S.; Walton, D. R. M. *J. Chem. Soc., Chem. Commun.* **1991**, 412−413.
(3) Hendra, P. J.; Jones, C.; Warnes, G. *Fourier Transform Raman Spectroscopy*; Ellis Horwood: Chichester, U.K., 1991.
(4) Meilunas, R.; Chang, R. P. H.; Liu, S.; Jensen, M.; Kappes, M. M. *J. Appl. Phys.* **1991**, *70*, 5128−5130.
(5) Bethune, D. S.; Meijer, G.; Tang, W. C.; Rosen, H. J.; Golden, W. G.; Seki, H.; Brown, C. A.; deVries, M. S. *Chem. Phys. Lett.* **1991**, *179*, 181−186.
(6) Dennis, T. J.; Hare, J. P.; Kroto, H. W.; Taylor, R.; Walton, D. R. M. *Spectrochim. Acta, Sect. A* **1991**, *47A*, 1289−1292.
(7) Chase, B.; Herron, N.; Holler, E. *J. Phys. Chem.* **1992**, *96*, 4262−4266.
(8) Procacci, P.; Cardini, G.; Salvi, P. R.; Schettino, V. *Chem. Phys. Lett.* **1992**, *195*, 347−351.
(9) van Loosdrecht, P. H. M.; van Bentum, P. J. M.; Meijer, G. *Phys. Rev. B* **1992**, *68*, 1176−1179.
(10) Tolbert, S. H.; Alivasatos, A. P.; Lorenzana, H. E.; Kruger, M. B.; Jeanloz, R. *Chem. Phys. Lett.* **1992**, *188*, 163−167.
(11) Xia, H.; Jiang, Q.; Tian, D. *Chem. Phys. Lett.* **1992**, *198*, 109−112.
(12) Chandrabhas, N.; Jayaram, K.; Muthu, D. V. S.; Sood, A. K.; Seshadri, R.; Rao, C. N. R. *Phys. Rev. B* **1993**, *47*, 10963−10966.
(13) Christides, C.; Nikolaev, A. V.; Dennis, T. J. S.; Prassides, K.; Negri, F.; Orlandi, G.; Zerbetto, F. *J. Phys. Chem.* **1993**, *97*, 3641−3643.
(14) Jishi, R. A.; Dresselhaus, M. S.; Dresselhaus, G.; Wang, K.; Zhou, P.; Rao, A. M.; Eklund, P. C. *Chem. Phys. Lett.* **1993**, 187−192.
(15) Shin, E.; Song, O.; Kim, D.; Suh, Y. D.; Yang, S. I.; Kim, S. K. *Chem. Phys. Lett.* **1994**, *218*, 107−114.
(16) Onida, G.; Andreoni, W.; Kohanoff, J.; Parrinello, M. *Chem. Phys. Lett.* **1994**, *219*, 1−7.
(17) Shinohara, Y.; Saito, R.; Kimura, T.; Dresselhaus, G.; Dresselhaus, M. S. *Chem. Phys. Lett.* **1994**, *227*, 365−370.
(18) Gallagher, S. H.; Armstrong, R. S.; Lay, P. A.; Reed, C. A. *Chem. Phys. Lett.* **1995**, *234*, 245−248.
(19) Lynch, K.; Tanke, C.; Menzel, F.; Brockner, W.; Scharff, P.; Stumpp, E. *J. Phys. Chem.* **1995**, *99*, 7985−7992.
(20) von Czarnowski, A.; Meiwes-Broer, K. H. *Chem. Phys. Lett.* **1995**, *246*, 321−324.
(21) Ajie, H.; Alvarez, M. M.; Anz, S. J.; Beck, R. D.; Diederich, F.; Fostiropoulos, K.; Huffman, D. R.; Krätschmer, W.; Rubin, Y.; Schriver, K. E.; Sensharma, D.; Whetten, R. L. *J. Phys. Chem.* **1990**, *94*, 8630−8633.
(22) Hare, J. P.; Kroto, H. W.; Taylor, R. *Chem. Phys. Lett.* **1991**, *177*, 394−398.
(23) Shumway, J.; Satpathy, S. *Chem. Phys. Lett.* **1993**, *211*, 595−600.

S0002-7863(96)03426-9 CCC: $14.00

Table 1. Comparison of Mode Assignments for Selected Raman Bands

band[a]	ref 24	ref 14	ref 26
228	E_2'	A_1'	E_2'
258	A_1'	E_2'	A_1'
399	A_1'	E_2'	E_1'
409	E_1''	E_2'	A_1'
455	A_1'	A_1', E_1''	A_1'
508	E_1''	E_2'	E_2'
569	A_1'	A_1', E_1''	A_1'
701	E_1''	E_2'	A_1'
714	E_2'	E_1''	E_2'
737	E_1''	A_1'	E_1'', A_1', E_2'
766	E_2'	E_1'', E_2'	E_1''
1062	A_1'	E_2'	A_1'
1165	E_2'	A_1'	E_1''
1182	E_1''	E_2', E_1''	A_1'
1227	E_2'	E_2', E_1''	A_1'
1257	E_1''	E_2', E_1''	E_1''
1296	E_1''	E_2'	E_2'
1313	E_2'	E_2'	—
1335	E_2'	E_2'	E_2'
1367	A_1'	E_2'	E_2'
1447	E_2'	E_2'	A_1'
1459	E_2'	E_1''	A_2'' (IR)
1469	E_1''	A_1'	A_1'
1493	E_2'	E_1''	E_2'
1515	E_1''	E_1'', E_2'	E_2'
1566	E_2'	E_2'	A_1'

[a] Listed frequencies are as reported in ref 14.

the similarity of their hemispherical "caps". Despite numerous studies on the Raman vibrational spectra of C_{70}, not all bands of the 53 possible Raman modes have been reported. A complete Raman (and infrared) vibrational assignment has yet to be made. Further, as shown in Table 1, there is little consistency of Raman mode assignments in the literature.[24,14,25]

We[18,25] and others[12,16,26] have commented on the problems associated with assigning bands to Raman vibrational modes of C_{70} on the basis of polarization data obtained from thin films. The symmetry-lowering effects of the surface can lead to unrepresentative data.[25] In addition, many studies have not considered that visible excitation leads to resonance, rather than normal, Raman scattering.[4,5,12,14,15,27,28] Such conditions produce marked variations in the intensities of Raman bands with different excitation energies for C_{70}.[18] Problems associated with the assignment of mode symmetries in C_{70} from thin films are discussed in this paper, and opposing assignments in the literature are clarified.

We also report the first Raman excitation profiles (REPs) for C_{70}. REPs are well-suited to probing the nature of the electronic transitions under an absorption envelope. In addition, REPs reveal the nature of the vibronic coupling and assist in the assignment of vibrational bands. The data lead to definitive assignments of the electronic transitions under the main visible absorption band (MVAB) where only tentative assignments have been made previously.[18,23] The four types of REPs provide valuable information on the nature of certain vibrational modes and their association with charge redistribution in certain electronic transitions.

Experimental Section

The resonance Raman (RR) spectra were obtained using two lasers. A Spectra Physics 2025-11 CW krypton ion laser provided the violet lines at 406.7 and 413.1 nm. A Spectra Physics 2025-05 CW argon ion laser provided nine blue-green lines at 454.5, 457.9, 465.8, 472.7, 476.5, 488.0, 496.5, 501.7, and 514.5 nm. Typical laser powers were 20−150 mW, depending on the power available for the excitation wavelength. The scattered light was focused with a Leitz *f*1.0 lens and collected at a 90° scattering geometry from the quartz spinning cell (∼2000 rpm). A polarization scrambler was used in all experiments to correct for the polarization bias of the Jobin-Yvon U1000 double monochromator (1800 grooves/mm gratings). Slit settings were 300 μm for all experiments. Calibration of the monochromator was performed using the mercury emission lines of the fluorescent lights in the laboratory.

Saturated solutions of C_{70} (prepared according to reported methods,[29] purity >99.6% by SALI mass spectrometry) were prepared in benzene (Merck, >99.5%) and CS_2 (Merck, >99.9%). The REP experiments were performed on the benzene solution at room temperature (∼20 °C). The resultant spectrum was the average of four runs at each wavelength, with 2-s integration times at each datum collection point (resolution of ±2 cm^{-1}) between 200 and 1650 cm^{-1}. No decomposition of C_{70} was detected from the first to the last runs. All resonance Raman spectra were uncorrected for baseline, and no smoothing was performed. Depolarization ratios were obtained using a polarizing filter aligned either parallel or perpendicular to the electric vector of the scattered light.

Fourier transform (FT) Raman spectra were recorded on a Bruker RFS 100 spectrometer with 1064-nm Nd:YAG laser excitation using a 1-cm pathlength cuvette. Spectra were the average of 1000 scans recorded at 2-cm^{-1} resolution for a benzene solution of C_{70} at the same concentration used in the REPs. The power at the sample was 100 mW.

To obtain the intensities and deconvolutions of Raman bands, band fits were performed using the GRAMS/386-based package.[30] Where there was convolution with other bands, band fit strategies involved using the same fit parameters for bands at each excitation. All band intensities were the average of three fits. The errors in absolute band intensities are indicated as error bars in the appropriate figures. The error in the depolarization ratios is ±0.10.

The method for the construction of the REPs is reported elsewhere.[31] The "ν^4" correction for the dependence of the intensity of the Raman band on the fourth power of the absolute energy was performed using three benzene solvent bands: at 605 cm^{-1} for the C_{70} bands at 250, 257, 570, 700, 713, 736, and 768 cm^{-1}; at 1178 cm^{-1} for the C_{70} bands at 1060, 1227, and 1256 cm^{-1}; and at 1568 cm^{-1} for the C_{70} bands at 1446, 1458, 1469, 1512, and 1566 cm^{-1}. The intensities of these benzene bands were also used for the self-absorption and optical path length corrections.

Results

The FT Raman experiment (i.e., normal Raman) on the benzene solution of C_{70} revealed only solvent bands. This means that the observation of bands due to Raman modes of C_{70} using visible excitation is a resonance effect. The positions of the laser lines relative to the electronic absorption spectrum of C_{70} in benzene are given in Figure 1 together with a Gaussian deconvolution of the visible bands. Figure 2 shows three typical RR spectra for the regions 200−650, 660−790, and 1050−1650 cm^{-1} at 514.1-, 476.5-, and 457.9-nm laser excitations, respectively. The REP constructions for the bands at 250, 257, 570, 700, 713, 736, 768, 1060, 1227, 1256, 1446, 1458, 1469, 1512, and 1566 cm^{-1} at the 11 laser excitation wave-

(24) Wang, X. Q.; Wang, C. Z.; Ho, K. M. *Phys. Rev. B* **1995**, *51*, 8656−8659.
(25) Gallagher, S. H.; Armstrong, R. S.; Lay, P. A.; Reed, C. A. *J. Raman Spectrosc.* **1997**, in press.
(26) Brockner, W.; Menzel, F. *J. Mol. Struct.* **1996**, *378*, 147−163.
(27) Wang, K.-A.; Zhou, P.; Rao, A. M.; Eklund, P. C.; Jishi, R. A.; Dresselhaus, M. S. *Phys. Rev. B* **1993**, *48*, 3501−3506.
(28) Bowmar, P.; Hayes, W.; Kurmoo, M.; Pattenden, P. A.; Green, M. A.; Day, P.; Kikuchi, K. *J. Phys.: Condens. Matter* **1994**, *6*, 3161−3170.
(29) Bhyrappa, P.; Penicaud, A.; Kawamoto, M.; Reed, C. A. *J. Chem. Soc., Chem. Commun.* **1992**, 936−937.
(30) Bio-Rad WIN-IR Version 2.04 based on GRAMS/386, Galactic Industries Corp., 1991−1993.
(31) Gallagher, S. H.; Armstrong, R. S.; Clucas, W. A.; Lay, P. A.; Reed, C. A. *J. Phys. Chem.* **1997**, *101*, 2960−2968.

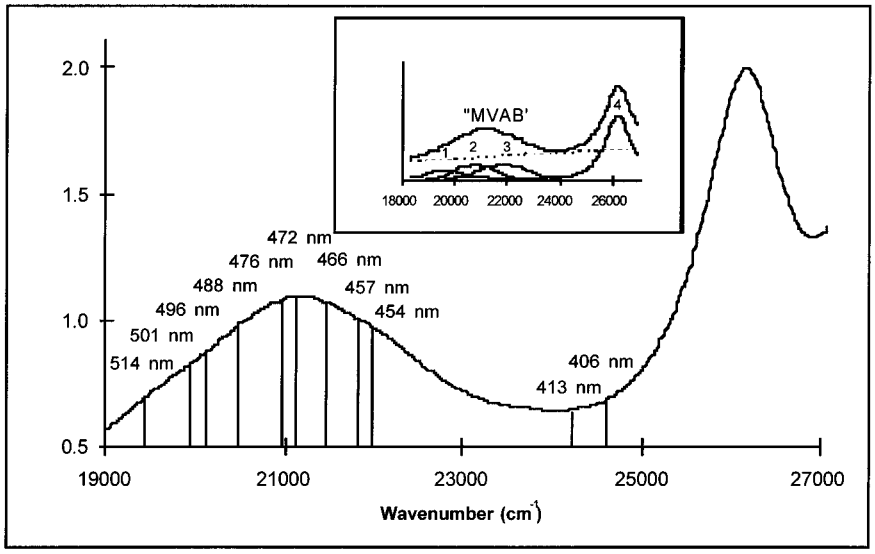

Figure 1. Positions of the laser lines relative to the electronic absorption spectrum of C_{70} in benzene. The inset shows the visible region absorption spectrum of C_{70} in benzene together with a Gaussian deconvolution.

lengths are given in Figures 3−5. It is clear that the REPs differ markedly for different bands.

Across the MVAB, there are three laser excitation regions at which the Raman bands have intensity maxima corresponding to bands 1, 2, and 3 of the deconvoluted spectrum shown in Figure 1. These regions are 514/501, 476/472, and 457/454 nm. Table 2 lists the wavelengths at which each of the Raman bands have their maximum intensity in the REP, along with secondary maxima, corresponding to bands 1, 2, and 3 of the deconvoluted spectrum shown in Figure 1. In the right hand column of Table 2 are the wavenumbers of the bands that have intensity at 413/406-nm laser excitations.

In general, the bands at <1000 cm^{-1} have lower absolute intensities than those at >1000 cm^{-1}. The four bands with the highest intensities in the REPs were those at 257, 1227, 1446, and 1556 cm^{-1}, respectively. Table 3 lists $\rho(\pi/2)$ values for the six most intense RR bands of C_{70} in benzene solution from this and previous work by us[18] and compares the results with thin film data of four other groups.[4,5,12,14] The other bands were too weak to obtain $\rho(\pi/2)$ values in solution. In addition to the 15 bands involved in the REPs, 10 other RR bands are reported in Table 4, which also contains assignments (see Discussion). The high-wavenumber region (>2000 cm^{-1}) was investigated for bands due to overtone and combination modes; however, no such features were evident.

Discussion

Assignment of C_{70} Raman Vibrational Modes. There are many papers in the literature that assign or report the Raman vibrational mode symmetries of C_{70} on the basis of theoretical[8,16,24,32−34] or experimental studies,[4,5,18] or both.[13−15,27,35,36] Of these, some have made assignments of the Raman vibrational mode symmetries of C_{70} partly on the basis of polarization data obtained from thin films in normal Raman scattering (*i.e.*, nonresonant) experiments. There are substantial inconsistencies in the reported $\rho(\pi/2)$ values (see Table 3). Three factors may contribute to these inconsistencies. First, the resonance conditions of each experiment have to be considered. The important factor is the degeneracy of the resonant electronic excited state. When the exciting laser line is in resonance with a nondegenerate or doubly-degenerate excited state of an electronic transition, the $\rho(\pi/2)$ values for bands due to totally-symmetric modes are $^1/_3$ or $^1/_8$, respectively, compared to a value of zero in the nonresonant case.[37] Second, for meaningful polarization data, either a random or highly-ordered orientation of molecules is required. Polycrystalline materials, such as thin films of C_{70}, are unlikely to satisfy either condition. Surface effects for thin films may cause varied orientation of C_{70} molecules, and the symmetry-lowering effects of boundary conditions cannot be ignored.[24] Third, there is evidence that two structurally similar phases of C_{70} coexist in thin films at room temperature.[38] Chandrabhas *et al.*[12] have shown that $\rho(\pi/2)$ values for all Raman bands of C_{70} from thin films are different at 14.3 and 296 K, a phenomenon that is associated with an orientational phase transition at ∼270 K. Thus, the variation in $\rho(\pi/2)$ values may also arise from phase differences in different experiments.

At the laser excitations used in these experiments, there are striking and unusual differences in resonance enhancement of the intensities of C_{70} Raman bands. The REPs highlight the inadequacies of experiments performed with visible radiation where resonance conditions have not been considered. There is even one report of intensity changes in the Raman spectrum of C_{70} that discounts resonance effects despite the use of laser wavelengths in the region of the MVAB.[28] In each of the thin film experiments reported in Table 3, the resonance conditions of the experiments were not considered, and clearly, the different excitation frequencies contribute to the large range of $\rho(\pi/2)$ values. Chandrabhas *et al.*[12] prudently did not make any assignments on the basis of their polarization work on thin films and noted the differences in the values of $\rho(\pi/2)$ between their work and that of Bethune *et al.*[5] They suggested that a systematic study of high-quality *single crystals* of C_{70} for such polarization work would be desirable. Recently, Fredericks[39]

(32) Slanina, Z.; Rudzinski, J. M.; Togasi, M.; Osawa, E. *J. Mol. Struct. (THEOCHEM)* **1989**, *202*, 169−176.
(33) Negri, F.; Orlandi, G.; Zerbetto, F. *J. Am. Chem. Soc.* **1991**, *113*, 6037−6040.
(34) Jishi, R. A.; Mirie, R. M.; Dresselhaus, M. S.; Dresselhaus, G.; Eklund, P. C. *Phys. Rev. B* **1993**, *48*, 5634−5641.
(35) Wang, Z. H.; Dresselhaus, M. S.; Dresselhaus, G.; Eklund, P. C. *Phys. Rev. B* **1993**, *48*, 16881−16884.
(36) Dresselhaus, M. S.; Dresselhaus, G.; Eklund, P. C. *J. Raman Spectrosc.* **1996**, *27*, 351−371.
(37) Clark, R. J. H.; Dines, T. J. *Angew. Chem., Int. Ed. Engl.* **1986**, *25*, 131−158.
(38) Ramasesha, S. K.; Singh, A. K.; Seshadri, R.; Sood, A. K.; Rao, C. N. R. *Chem. Phys. Lett.* **1994**, *220*, 203−206.
(39) Fredericks, P. M. *Chem. Phys. Lett.* **1996**, *253*, 251−256.

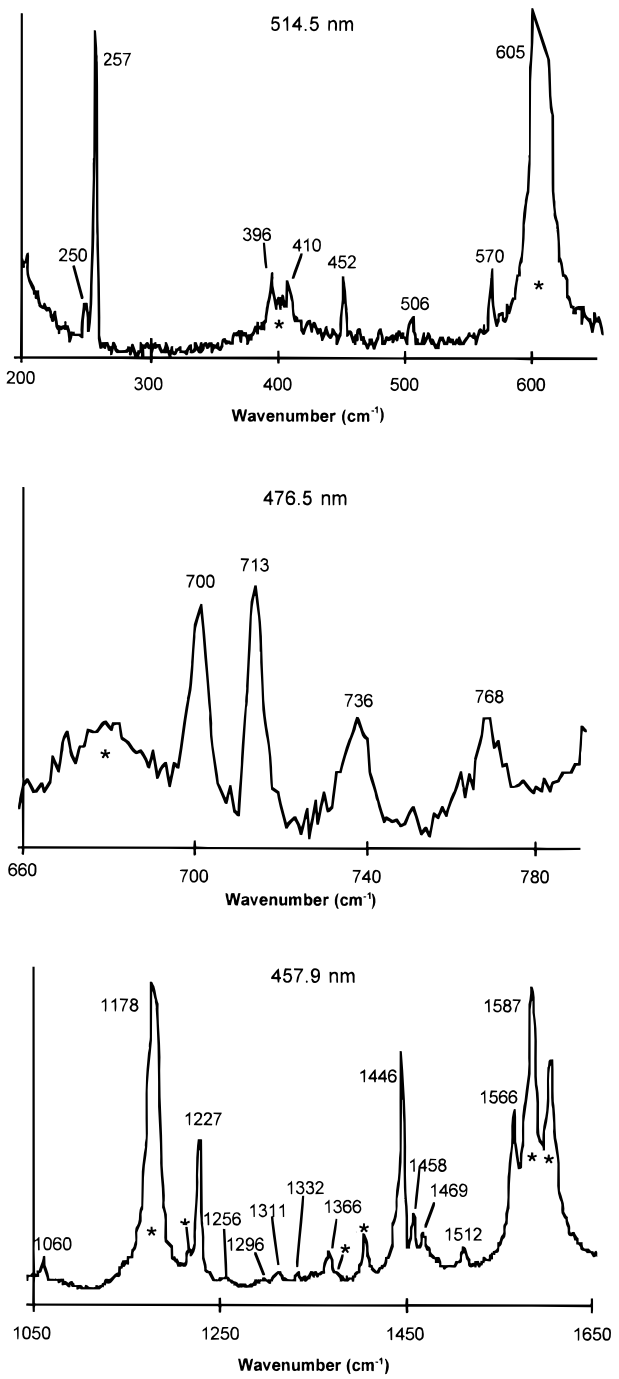

Figure 2. RR spectrum of a saturated solution of C_{70} in benzene in the 200−650-cm^{-1} region at 514.5-nm excitation, in the 660−790-cm^{-1} region at 476.5-nm excitation, and in the 1050−1650-cm^{-1} region at 457.9-nm excitation. Solvent peaks are marked with an asterisk.

reported that the excitation wavelength has a large effect on the intensity of some bands in the surface-enhanced Raman (SER) spectrum of thin films of C_{70}. Clearly, symmetry assignments of bands of C_{70} Raman modes derived from studies on thin films must be seriously questioned.

Solution measurements overcome the difficulties associated with thin films. The assignments reported herein are based on results of measurements of $\rho(\pi/2)$ for six intense bands in the RR spectrum of C_{70} in benzene.[18] The $\rho(\pi/2)$ values are consistent with most of the predictions of Wang *et al.*[24] for the Raman mode symmetries listed in Table 4. These assignments are in accord with most of the assignments of Meilunas *et al.*,[4] Procacci *et al.*,[8] Onida *et al.*,[16] and Christides *et al.*,[13] and they clarify ambiguities in assignments previously made to modes of E_1''/E_2' symmetries.[8,18] They are not in accord with those of Shin *et al.*[15] nor those in a series of papers by Dresselhaus and co-workers,[14,27,35,36] where the problems associated with thin films and resonance conditions were not addressed. Very recently, Brockner and Menzel[26] attempted a complete assignment of the observed bands to vibrational modes using "genetic" relationships between C_{60} and C_{70} in conjunction with semi-empirical PM3 calculations. However, this first attempt to provide a comprehensive treatment of the modes of C_{70} has led to incorrect mode assignments for the bands at 396, 410, 506, 769, 1256, 1296, 1333, 1366, 1458, and 1566 cm^{-1} and uncertain assignments for the 738- and 1311-cm^{-1} bands (see below).

Scattering Mechanisms, Vibronic Coupling, and Assignments of Electronic Transitions. The three-dimensional cage structures of fullerenes make them distinct from most other classes of molecules. Vibrationally, there are no discrete vibrating units, and consequently, vibrational modes of fullerenes are described by the tangential or radial motion of the atoms.[13,17,34] This connectivity of the fullerene frame is also important for their resonance Raman scattering. A-term RR scattering is usually the dominant scattering mechanism for totally-symmetric modes.[37] Vibrational modes that have the same vibrational coordinates as the displacement of the molecular geometry in the excited state will have their band intensities enhanced by A-term scattering. The nuclear displacement, ΔQ, of the potential surface of the excited electronic state minimum from that of the ground electronic state is defined as

$$\Delta Q = \mu^{1/2}\Delta S \tag{1}$$

where μ is the reduced mass associated with the vibration and ΔS is the corresponding displacement along the relevant symmetry coordinates. It is related to the change in bond lengths Δr by

$$\Delta S = \frac{1}{\sqrt{n}}(\Delta r_1 + ... + \Delta r_n) \tag{2}$$

where n is the number of bonds involved with the vibration. A totally-symmetric vibration of C_{70} would involve most of the 105 bonds. On the basis of calculations[40] of the changes in the bond lengths from C_{70} to C_{70}^{2-}, the weighted average change for all bonds is ~0.01 Å. It is expected that Δr associated with electronic excitation would be significantly smaller. Hence, ΔQ becomes exceedingly small and would preclude any significant contributions from "small displacement" A-term scattering. Systems in which "small displacement" A-term scattering is significant include the linear ruthenium reds and browns, which have no strongly-allowed transitions in the proximity of the resonant transition.[41] As for C_{60}, the negligible A-term scattering leads to the expectation that vibronic coupling mechanisms involving B-term scattering will be the major source of intensity enhancement for bands that result from the totally-symmetric A_1' modes of C_{70}. It is also the main enhancement mechanism for those that result from the non-totally-symmetric E_1'' and E_2' modes.[31,42,43] Via this mechanism, bands of modes of the appropriate symmetry that couple the resonant electronic excited state with a second nearby excited state gain intensity through the mixing of the two excited states. It is generally a valid assumption that only one excited state is coupled to the

(40) Roduner, E.; Reid, I. D. *Chem. Phys. Lett.* **1994**, *223*, 149−154.
(41) Clark, R. J. H.; Dines, T. J. *Mol. Phys.* **1981**, *42*, 193−207.
(42) Gallagher, S. H.; Armstrong, R. S.; Lay, P. A.; Reed, C. A. *J. Am. Chem. Soc.* **1994**, *116*, 12091−12092.
(43) Gallagher, S. H.; Armstrong, R. S.; Lay, P. A.; Reed, C. A. *Chem. Phys. Lett.* **1996**, *248*, 353−360.

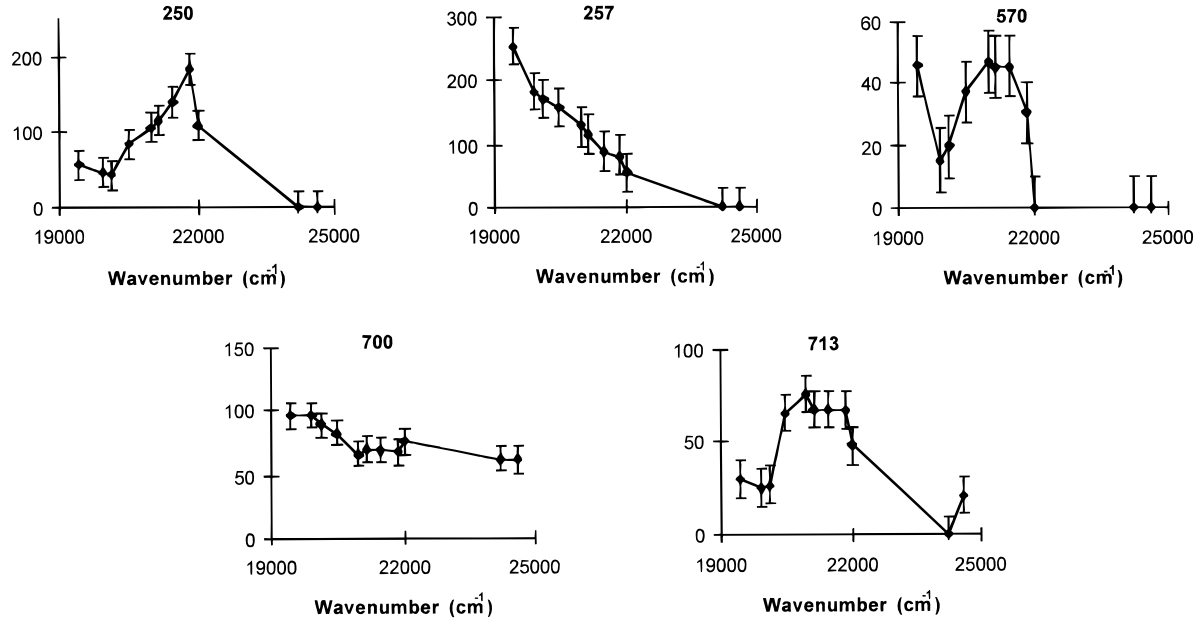

Figure 3. Raman excitation profile for the RR bands at 250, 257, 570, 700, and 713 cm^{-1} for C_{70} in benzene at the 11 laser lines shown Figure 1.

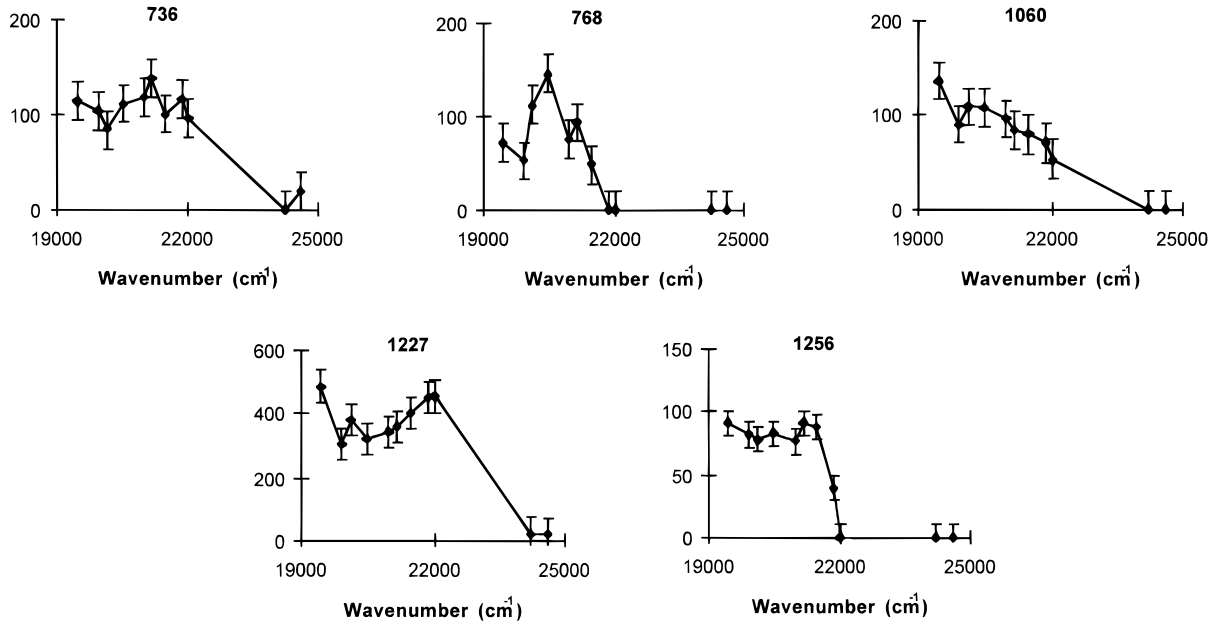

Figure 4. Raman excitation profile for the RR bands at 736, 768, 1060, 1227, and 1256 cm^{-1} for C_{70} in benzene at the 11 laser lines shown Figure 1.

resonant excited state.[37,44] For C_{70}, all of the electronic states involve MOs of a_1, e_1, or e_2 symmetry. Table 5 gives the symmetries of the vibrational modes capable of coupling specific electronic states of D_{5h} C_{70}. Symmetry considerations of vibronic coupling, therefore, provide considerable insight into the nature of the electronic transitions of C_{70} contributing to the MVAB and, when used in combination with depolarization ratios, allow assignments of these electronic transitions to be made. The $\rho(\pi/2)$ values for bands of the totally-symmetric A_1' modes at 457.9-, 476.5-, and 514.5-nm excitations (Table 3) provide accurate information about the symmetry of the resonant excited state. At 476.5- and 514.5-nm excitation, $\rho(\pi/2)$ values are close to $^1/_8$ for the bands of the A_1' modes at 257, 1227, and 1446 cm^{-1}. This is strong evidence that doubly-degenerate excited states are populated at these excitations. At 457.9-nm excitation, however, the $\rho(\pi/2)$ value for the band of the A_1' mode at 1227 cm^{-1} is $\sim^1/_3$, while it remains $\sim^1/_8$ for the 1446-cm^{-1} band. Clearly, these two values for $\rho(\pi/2)$ indicate that there are two electronic transitions being probed by the 457.9-nm line, with excited states of a and e orbital symmetry, respectively. The 1227-cm^{-1} vibration is active in the vibronic coupling of the excited states with a orbital symmetry but not with orbitals of e symmetry. The converse is true for the 1446-cm^{-1} vibration.

It is assumed that a RR band active in vibronic coupling has its maximum intensity at an excitation closest to the absorption maximum of the corresponding resonant electronic transition. Generally, various bands of the A_1' and E_2' modes have their highest intensities in both 514/501- and 476/472-nm excitation regions, while bands of the E_1'' modes have their highest intensities in the 457/454-nm excitation region (Table 2). From the direct products in Table 5, for both A_1' and E_2' modes to be active in vibronic coupling of the same resonant electronic

(44) Clark, R. J. H.; Stewart, B. *Struct. Bonding (Berlin)* **1979**, *36*, 1−80.

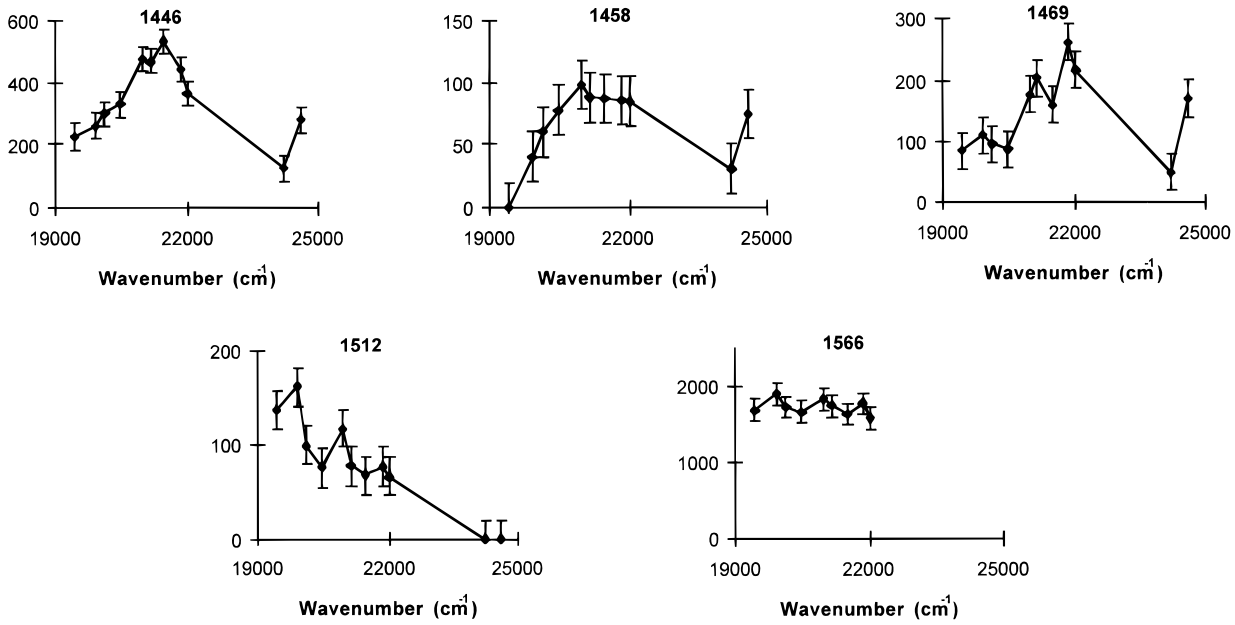

Figure 5. Raman excitation profile for the RR bands at 1446, 1458, 1469, 1512, and 1566 cm^{-1} for C_{70} in benzene at the 11 laser lines shown Figure 1. The REP of the 1566-cm^{-1} band does not include 413- and 406-nm excitations due to the solvent band coincidence and the weak intensity of the Raman bands at resonance with these excitations.

Table 2. Maxima and Relative Intensities of REPs[a]

514.5/501.7 nm	476.5/472.7 nm	457.9/454.5 nm	413.1/406.7 nm
	Primary Maxima		Band
257	570	250	452
700	713	1469	700
1060	736		713
1227	1446		736
1256	1458		1060[b]
1512			1227
1566			1311[b]
	Secondary Maxima		1366
250	1256	1227	1446
570	1512		1458
713			1469
736			1512[b]
1469			1566[c]

[a] The first three columns give the laser excitation energies at which each band (cm^{-1}) in the REP has its greatest intensity and also any secondary maxima. The fourth column gives the bands that have intensity at 413.1/406.7-nm excitation. [b] These bands did not have sufficient intensity at these excitations for band fits to be performed for the REPs, but they have non-zero intensities at these excitations. [c] This band is obscured by benzene solvent bands, but at these excitations, it is evident with CS_2 as the solvent.

transition, both the resonant and coupled electronic excited states must involve MOs of e_1 symmetry. Calculations of Shumway and Satpathy[23] suggest that the electronic transition in the 476/472-nm excitation region corresponding to the excited state of e_1 orbital symmetry is the *z*-polarized HOMO − 5 (e_1') → LUMO + 1 (e_1''). This assignment was determined in preliminary experiments[18] and has been reaffirmed by the more extensive data reported in this work. Hereafter it is referred to as transition **2**. The excited state of the electronic transition in the 514/502-nm excitation region also involves an orbital of e_1 symmetry, and on the basis of the molecular orbital scheme of Shumway and Satpathy,[23] the candidate transition at this energy is the *x*,*y*-polarized HOMO − 4 (e_2'') → LUMO + 1 (e_1'') (transition **1**), which is consistent with the depolarization ratios.

The $\rho(\pi/2)$ value of the 1227-cm^{-1} band at 457.9-nm excitation is the manifestation of a nondegenerate excited state of the resonant transition. In addition to transition **2**, Shumway and Satpathy[23] predict that another *z*-polarized transition may occur at a similar energy, the HOMO (a_2'') → LUMO + 2 (a_1'') (transition **3**). This transition has a nondegenerate excited state and is assigned to the resonant transition in the 457/454-nm excitation region. The E_1'' vibrational modes have their highest intensity in this excitation region, and from group theory, they couple the resonant excited state of a_1 orbital symmetry to an excited state of e_1 orbital symmetry.

The question now arises as to which excited state(s) the three electronic transitions, **1**, **2**, and **3**, are coupled. The candidate excited state(s) for coupling will be energetically close. For *B*-term scattering mechanisms to operate for totally-symmetric modes, the excited states of both the resonant and coupled transition are required to be of the same symmetry. Thus, the excited states of transitions **1** and **2** are vibronically coupled with a second excited state of e_1 orbital symmetry, based on the REPs of the bands of the A_1' modes. The excited state of transition **3** is also coupled to an excited state of e_1 orbital symmetry based on the REPs of the bands of the E_1'' modes. Referring to the MO scheme of Shumway and Satpathy,[23] the *x*,*y*-polarized HOMO − 2 (a_2') → LUMO + 3 (e_1') transition **4** satisfies both symmetry and energy requirements and is assigned to the strong absorption band at 382 nm.

Where the coupled electronic transitions have similar oscillator strengths, a second band intensity maximum of the coupling vibration is expected upon resonance within the absorption envelope of this "second" electronic transition. Such behavior is evidenced in the REPs of manganese porphyrins.[45] Inspection of the intensity enhancements in the 413/406-nm excitation region (Table 2) reveals that many of the bands due to modes of A_1', E_1'', and E_2' symmetries involved in the vibronic coupling of transitions **1**, **2**, or **3** also have enhanced intensity upon resonance with the low-energy tail of transition **4**. It could be argued that this RR intensity is due to resonance with the tails of the absorption envelopes of transitions **1**, **2**, or **3**. If this were the case, such a phenomenon would be manifested in greater intensities at 413-nm excitation. However, it is clear from the REPs that most bands have a greater intensity at 406 than at 413-nm excitation and that all bands have at least equal

(45) Foran, G. J. Ph.D. Thesis, University of Sydney, 1993.

Table 3. Depolarization Ratios, $\rho(\pi/2)$, for C_{70}

band (cm^{-1})	this work,[a] 457 nm, RT	ref 18,[a] 476 nm, RT	ref 18,[a] 514 nm, RT	ref 14,[b] 488 nm, RT	ref 12,[c] 514 nm, 296.0 K	ref 12,[c] 514 nm, 14.3 K	ref 5,[d] 514 nm, RT	ref 4,[e] 514, 488 nm, RT
257	*f*	0.09	0.08	0.33	0.39	0.30	0.16	0.24
738	*f*	0.84	0.82	0.38	0.54	1.12	0.39	0.75
1227	0.29	0.19	0.10	0.37	0.35	0.52	0.16	0.2
1256	*f*	0.90	0.80	0.87	0.89	0.97	—	0.62
1446	0.18	0.16	0.15	0.40	0.41	0.21	0.17	0.23
1566	0.66	0.60[g]	0.63[g]	0.19	0.61	0.39	0.19	0.29

[a] Benzene solution. RT = room temperature. [b] Microcrystalline films deposited on CsI substrate by vacuum sublimation. [c] Films deposited on single crystals of Si(100) by vapor-pressure gradient method of Varma *et al*. (Varma, V.; Seshadri, R.; Govindaraj, A.; Sood, A. K.; Rao, C. N. *Chem. Phys. Lett.* **1993**, *203*, 545−548). [d] Films deposited on suprasil slides by vacuum sublimation. [e] Films deposited by vacuum sublimation onto Si(100) substrates. [f] Insufficient band intensity. [g] This work.

Table 4. Symmetry Assignments of the Vibrational Modes Giving Rise to the Resonance Raman-Active Bands (cm^{-1}) of C_{70}[a]

A_1'	E_1''	E_2'
257	250	233
452	410	396
569	506	714
701	1296	738
1060	1333	769
1227	1468	1256
1366		1311
1446		1458
		1512
		1566

[a] Bands observed in benzene solution, this work.

Table 5. Direct Product Table Involving Electronic Excited State Symmetries for the D_{5h} Point Group

⊗	a_1	e_1	e_2
a_1	a_1	e_1	e_2
e_1		$a_1 + e_2$	e_1
e_2			$a_1 + e_1$

intensity at both excitations. This is consistent with the proposed coupling of the excited states of transitions **1**, **2**, and **3** with transition **4**.

The occurrence of secondary maxima for A_1' and E_2' modes in the 514/501- and 476/472-nm excitation regions (Table 2) is due to vibronic coupling of transition **1** or **2** with transition **4** by that vibrational mode. The lower intensity of the secondary maxima of these modes is a reflection of their association with a different change in the electronic distribution upon excitation. There is a secondary maximum for the A_1' 1227-cm^{-1} band in the 457/454-nm excitation region. As evidenced by the depolarization ratio, this band gains intensity upon resonance with the excited state of transition **3** having an MO of a_1'' symmetry and is active in the vibronic coupling of this excited state with another excited state of like orbital symmetry.

The REPs of most RR bands of C_{70} have intensities in excitation regions where they are not involved in vibronic coupling of the dominant resonant transition in that excitation region. For example, the 250- and 1469-cm^{-1} bands of the E_1'' modes in the 514/501-nm excitation region have low intensities. Studies on the solvatochromism of the electronic absorption spectrum of C_{70} revealed that the position of the peak of the MVAB is insensitive to the nature of the solvent, unlike other electronic bands, e.g., the peak of the band due to transition **4**.[46] This suggests that no electronic transition dominates the MVAB, but instead that transitions **1**, **2**, and **3** most likely have comparable probabilities. The absorption profiles of transitions

(46) Gallagher, S. H.; Armstrong, R. S.; Bolskar, R. D.; Lay, P. A.; Reed, C. A. *Recent Advances in the Chemistry and Physics of Fullerenes and Related Materials*; Electrochemical Society: Pennington, NJ, 1995; Vol. 95−10, pp 485−498.

Table 6. Bands (cm^{-1}) Belonging to the Four Types of REPs[a]

type 1	type 2	type 3	type 4
257 A_1'	570 A_1'	250 E_1''	1446 A_1'
700 A_1'	713 E_2'	1469 E_1''	1458 E_2'
1060 A_1'	736 E_2'		
	768 E_2'		
	1256 E_2'		
	1512 E_2'		

[a] See text for discussion. Bands at 1227 and 1566 cm^{-1} do not fit into any of these types.

1, **2**, and **3** will overlap given their proximity to each other. Therefore, the decreasing intensities of many bands across the MVAB away from their resonance maximum are due to resonance with the tails of transitions **1**, **2**, or **3**.

Association of Raman Vibrational Modes of C_{70} with the Electronic Distribution. As the previous section has demonstrated, symmetry arguments allow for detailed investigation and the assignment of electronic transitions under the MVAB. However, such arguments fail to address why vibrational bands of modes of the same symmetry display remarkably different REPs. The constructed REPs of the 15 bands can be divided into the four types given in Table 6. Type 1 bands have one maximum in the 514/501-nm excitation region and tail off in intensity toward the 457/454-nm excitation region. Type 2 bands have maxima in both 514/501- and 476/472-nm excitation regions. Type 3 and 4 bands have maxima in 457/454- and 476/472-nm excitation region, respectively. Therefore, type 1 bands have a maximum upon resonance with transition **1**; type 2 have maxima upon resonance with transitions **1** and **2**; type 3 have maxima upon resonance with transition **3**; and type 4 have a maximum upon resonance with transition **2**. The 1227- and 1566-cm^{-1} bands do not fit into any of these types. These different types of REPs are now discussed in terms of the changes in the electronic distribution upon excitation. This requires a more detailed understanding of both the frontier molecular orbitals and of the nature of the fundamental vibrational modes of C_{70} for the 738- and 1311-cm^{-1} bands, cf. Tables 1 and 4.

As with C_{60}, the vibrational modes of C_{70} can be distinguished as either radial (changes in bond angles) or tangential (changes in bond lengths); these generally occur at $<\sim$900 and $>\sim$900 cm^{-1}, respectively.[13,17,34] However, the extra 10 carbon atoms in C_{70} allow a further distinction: modes involved with the C_{60}-like hemispheres are "cap" modes, while those involved with the equatorial region are "belt" modes; the latter are characteristic vibrations of C_{70}. Strictly speaking, there are no pure belt and pure cap modes because of extensive mixing of modes with like symmetry. Of the 53 Raman-active modes of C_{70}, Jishi *et al*.[34] predict eight belt and 45 cap modes.

There is little known about the nature of the Raman fundamental modes of C_{70}. Onida *et al*.[16] have suggested assignments based on calculations, which are in good agreement

with the inelastic neutron scattering experiments of Christides *et al.*[13] The only Raman modes they identify with confidence are the three low energy modes that correspond to the band of the 5-fold degenerate $H_g(1)$ squashing mode of C_{60} at 264 cm^{-1} in solution.[31,43] These are the bands due to the E_2' mode at 235 cm^{-1} and two accidentally degenerate bands at 250 cm^{-1}, corresponding to the E_1'' and A_1' modes. Christides *et al.*[13] give the band positions of the E_2', E_1'', and A_1' modes as 233, 252, and 266 cm^{-1}, respectively, and on the basis of the experimental work reported here, they correspond to the bands of the E_2' mode at 233 cm^{-1}, the E_1'' mode at 250 cm^{-1}, and the A_1' mode at 257 cm^{-1}. Onida *et al.*[16] have identified that the analogous vibrations of the $A_g(1)$ breathing mode and $A_g(2)$ pentagonal pinch modes of C_{60} are the two A_1' modes of C_{70}, with calculated energies of 465 and 1463 cm^{-1}, respectively. They most probably correspond to the bands at 452 and 1446 cm^{-1} found here. Onida *et al.*[16] predict only one Raman-active mode characteristic of C_{70}, the vibration at 1552 cm^{-1}, found in the present work at 1566 cm^{-1}. Given the energy of this band, this would correspond to a tangential mode, i.e., a breathing mode of the belt.

The HOMO and LUMO of C_{60} are delocalized over the whole molecule, owing to the icosahedral symmetry. In contrast, the LUMO and LUMO + 1 of C_{70} are essentially delocalized to first-order approximation over 40 and 46 carbon atoms, respectively.[23,47] In this discussion, we have adopted the C_{70} carbon-labeling method of Roduner and Reid.[40] The 10 carbon atoms of the equatorial belt are labeled C_E, and the four successive bands from the equator to the poles are labeled from C_D to C_A, such that the C_A carbons form the polar pentagonal caps. Calculations predict that population of the LUMO has the same effect on the electronic distribution as removing electrons from the HOMO,[40] such that population of the LUMO results in a net positive charge for the C_E carbons, while all other carbons have a net negative charge.[40,48] This negative charge is greatest for the C_D carbons and decreases for each band toward the poles.[40] There are nodes at the 10 C_A carbon atoms of both poles[23,47] and at the 10 C_E carbon atoms in the equatorial belt.[23] It is also calculated that the three highest HOMOs (HOMO, HOMO − 1, HOMO − 2) and the three lowest LUMOs (LUMO, LUMO + 1, LUMO + 2) of C_{70} have a nodal plane through the C_E carbons.[40] Hence, any electronic transition that has one of the three HOMOs as its origin and/or populates one of the three LUMOs effectively moves electronic distribution in a direction parallel to the long axis of C_{70}. Specifically, for an electron hole created in the HOMO or HOMO − 1, electronic distribution moves toward the C_E carbons, while it moves away from the C_E carbons upon population of the LUMO or LUMO + 1.[40] The change in the electronic distribution upon excitation, therefore, is defined by the electron hole created and the destination of that electron, *i.e.*, the "origin" and "populated" orbitals, respectively. On the basis of the assignments made for transitions **1**, **2**, and **3**, the electron hole is different for each, the HOMO − 4 (e_2''), HOMO − 5 (e_1'), and HOMO (a_2''), respectively. However, for both transitions **1** and **2**, the populated orbitals are the same, that being the LUMO + 1 (e_1''), whereas the populated orbital for transition **3** is the LUMO + 2 (a_1'').

In general, the bands of tangential modes $>\sim$900 cm^{-1} have greater intensities than those of the radial modes at $<\sim$900 cm^{-1}, with the notable exceptions being the 250- and 257-cm^{-1} bands. This suggests that the higher energy modes modulate more effectively the change in the electronic distribution upon excitation than do the radial modes. The positively identified modes of C_{70} in this work include the low-energy bands at 250 and 257 cm^{-1} due to the E_1'' and A_1' modes, respectively. They are related to the $H_g(1)$ squashing mode of C_{60} and thus will be both radial and "cap" in nature. Onida *et al.*[16] have assigned the lowest frequency mode at 235 cm^{-1} to E_2' symmetry, implying that it is easier to squash the molecule perpendicular to the *long* axis than along it. In this work, the band at 233 cm^{-1} most likely corresponds to this lowest energy E_2' mode. It has weak intensity only at 457.9-nm excitation, *i.e.*, upon resonance with transition **3**, and is not evident elsewhere. Intuitively, the higher energy of the E_1'' mode at 250-cm^{-1} suggests that this squashing mode is perpendicular to the *short* axis. The 250-cm^{-1} E_1'' band has a REP of type 3, with an intensity maximum upon resonance with transition **3**. Referring to the change in the electronic distribution associated with transition **3**, the change occurs along the long axis and not perpendicular to it. Hence, the nature of the 250-cm^{-1} E_1'' mode modulates this change in the electronic distribution. In contrast, the E_2' mode symmetry of the 233-cm^{-1} band is capable of vibronically coupling the excited states of transitions **1** and **2**, yet, as it has a weak intensity, this vibration modulates the electronic distribution perpendicular to the change in the electronic distribution associated with the excitation. While the assignments of these low-energy bands are consistent with the predictions of Onida *et al.*[16] many of our assignments of the higher energy bands differ from the most recent compilation by Brockner and Menzel.[26,49] As the band of the E_1'' mode at 1469 cm^{-1} has the same excitation profile as the 250-cm^{-1} band, the nature of the high-energy vibration is similar to that of the low-energy vibration. Without knowing the exact nature of the 257-cm^{-1} mode, it is difficult to speculate as to how this totally-symmetric vibration might modulate the electronic distribution. However, it has a REP of type 1 along with the bands due to the A_1' modes at 700 and 1060 cm^{-1}, suggesting that the change in the electronic distribution upon resonance with transition **1** may also be totally-symmetric in nature. The same may be said about REPs of type 2 vibrational bands. The vibrations which have these excitation profiles will yield a great deal of information about the associated electronic transitions once the nature of each of the vibrations of type 2 are known.

The bands at 452 and 1446 cm^{-1} assigned to the two A_1' modes, identified as the analogous C_{70} vibrations to the breathing and pentagonal pinch modes of C_{60}, respectively,[16] have remarkably different excitation responses. Surprisingly, the 452-cm^{-1} band does not have sufficient intensity at laser excitations across the MVAB to allow construction of a REP. In contrast, the 1446-cm^{-1} band has the second highest absolute intensity of the C_{70} bands studied in this work. To a lesser extent, this intensity relationship is also observed for the two A_g modes of C_{60}.[31] The 1446-cm^{-1} band has a REP of type 4 with an intensity maximum upon resonance with transition **2**. Mindful of the proposed node at the equator for the populated orbital of transition **2**,[40] the REP of this band suggests that transition **2** also produces a change in the electronic distribution associated with the pentagons in the caps. The band of the 1458-cm^{-1} E_2' mode also has a type 4 excitation profile and, thus, is predicted to modulate the electronic distribution in a manner similar to that of the 1446-cm^{-1} band.

Conclusion

The REPs of the intense RR bands of C_{70} across the visible region require that depolarization experiments must consider

(47) Haddon, R. C. *J. Am. Chem. Soc.* **1996**, *118*, 3041−3042.
(48) Tanaka, K.; Matsuura, Y.; Oshima, Y.; Yamabe, T. *Chem. Phys. Lett.* **1995**, *237*, 127−132.
(49) Gallagher, S. H.; Armstrong, R. S.; Bolskar, R. D.; Lay, P. A.; Reed, C. A. *J. Mol. Struct.* **1997**, *406*, in press.

any resonance effects and that either a random orientation or highly-ordered array of molecules is a prerequisite for meaningful results. With few exceptions, the present work is consistent with the vibrational assignments of Wang *et al.*[14] The REPs also reveal that there are three electronic transitions which contribute to the MVAB and definitive assignments have been made for the first time. Each of these is vibronically coupled to the strongly-allowed transition at ~380 nm.

B-term scattering is the dominant scattering mechanism for C_{70}. This arises from extensive vibronic coupling and from the rigidity of a highly connected structure where there are no discrete vibrating units. A-term contributions are small, if not negligible, even upon resonance for strongly-allowed transitions. These observations for C_{70} are expected to translate predictively to the higher fullerenes. Because C_{70} has lower symmetry and more localized molecular orbitals than C_{60}, it is a superior model for the vibrational dynamics and vibronic coupling of higher fullerenes.

Acknowledgment. The authors are grateful for support from the Australian Postgraduate Award Scheme (S.H.G.), the Australian Research Council (R.S.A. and P.A.L.) and the National Institutes of Health (GM 23851) (C.A.R.). The assistance of Dr B. M. Collins with the calibration of REP data is gratefully acknowledged.

JA963426F